


 Cite this: *RSC Adv.*, 2024, **14**, 8124

Study on the structure–activity relationship of cationic polyacrylates for the treatment of oilfield produced water

 Zhiping Chen,^a Xiuju Wang,^{bc} Jian Zhang,^{bc} Wenju Zhang,^a Ming Duan,^{id} ^{*a}
 Yan Xiong^a and Shenwen Fang^{ad}

Cationic polyacrylates exhibit both reverse demulsification and flotation performance, which can avoid incompatibility between the reverse demulsifier and flotation agent during treatment of produced water from offshore oilfields. In our previous work, the effect of the structure of the cationic unit on the reverse demulsification and flotation performance of cationic polyacrylates was studied. However, the structure–activity relationship of cationic polyacrylates has not been systematically studied. In this study, the relationships between the structure (acrylate type, tertiary amine type, mass ratio of acrylate to tertiary amine, and degree of cationicity), interfacial properties (surface tension, interfacial tension, zeta potential, interfacial elastic modulus, interaction force between oil droplets, and film drainage time of an oil-covered bubble), and reverse demulsification and flotation performance of cationic polyacrylates were investigated. A reduction in the elastic modulus of the oil–water interface was the key factor for good reverse demulsification performance, whereas a decrease in the film drainage time of an oil-covered bubble was the key factor for good flotation performance. Ethyl acrylate (EA) was superior to methyl acrylate (MA), and dimethylaminopropyl methacrylamide (DPM) was superior to dimethylaminoethyl methacrylate (DEM). Increases in the mass ratio of ethyl acrylate to dimethylaminopropyl methacrylamide and the degree of cationicity were beneficial for reducing the elastic modulus of the oil–water interface and the film drainage time of an oil-covered bubble. This is the first time that the structure–property–performance relationship of cationic polyacrylates has been systematically studied. A cationic polyacrylate that exhibited both good reverse demulsification performance and good flotation performance is recommended.

 Received 8th January 2024
 Accepted 5th March 2024

 DOI: 10.1039/d4ra00188e
rsc.li/rsc-advances

1. Introduction

Currently, some offshore oilfields have entered the middle and late stages of exploitation, and the water content of produced fluids is increasing. In general, produced fluids from offshore oilfields are treated using three-phase separation, thermal processing, and electric dehydration to obtain anhydrous crude oil, while a large amount of oily wastewater (also referred to as produced water) is generated.^{1–4} The produced water is treated by inclined-plate separation, flotation, and walnut shell filtration and is then reinjected into the formation. In order to remove oil more efficiently, a reverse demulsifier is added to the three-phase separator to remove large oil droplets from water,⁵

and a flotation agent is added to the flotation separator to remove small oil droplets from water.⁶

Two types of reverse demulsifiers are used in offshore platforms: (1) cationic polymers, such as hyperbranched poly(amide amine)⁷ and cationic polyacrylamide,^{8,9} which can destabilize oil droplets in water by reducing their zeta potential; and (2) nonionic block polyethers, such as block copolymers of ethylene oxide (EO) and propylene oxide (PO) prepared by anionic polymerization of EO and PO using polyethylenimine and *N,N*-dimethylethanolamine as the acceptor,^{10,11} which can destabilize oil droplets in water by reducing the strength of the oil–water interfacial film. In addition, there are also two main types of flotation agents: (1) low-molecular-weight cationic surface-active compounds, such as dodecyltrimethylammonium chloride and cetyltrimethylammonium bromide, which can provide good oil removal performance by increasing the adhesion efficiency of oil droplets and bubbles;¹² and (2) high-molecular-weight cationic surface-active compounds, such as polytriethanolamine modified with quaternary ammonium salts and copolymers of tertiary amines and quaternary ammonium monomers, which can provide good oil removal performance by increasing the collision

^aSchool of Chemistry and Chemical Engineering, Southwest Petroleum University, 8 Xindu Avenue, Xindu District, Chengdu, Sichuan, 610500, China. E-mail: [swpu124@126.com](mailto:swpua124@126.com); Fax: +86-2883037346; Tel: +86-2883037346

^bState Key Laboratory of Offshore Oil Exploitation, Beijing, China

^cCNOOC Research Institute Company, Ltd, Beijing, China

^dIndustrial Hazardous Waste Disposal and Resource Utilization Research Institute, Southwest Petroleum University, Chengdu, Sichuan, China



efficiency of oil droplets and bubbles.^{13,14} Ensuring high compatibility between the reverse demulsifier and flotation agent is one of the issues that need to be considered in the treatment of produced water from offshore platforms. For example, when a nonionic block polyether was used as the reverse demulsifier, residual polyether was adsorbed onto the oil–water interface and had a negative effect on the adhesion efficiency of oil droplets and bubbles. Therefore, a larger amount of the flotation agent was needed. If the reverse demulsifier and flotation agent are in the same class, in particular, if the same treatment agent can exhibit both reverse-phase demulsification and flotation performance, it would be ideal if residual reverse demulsifier could be used as a flotation agent. In our previous work, we found that cationic polyacrylates are capable of both reverse demulsification and flotation, and the effect of the cationic unit on their performance was investigated.¹⁴ However, there is still a lack of systematic studies of the structure–property–performance relationship of cationic polyacrylates. In this study, the effects of acrylate type, tertiary amine type, mass ratio of the acrylate to the tertiary amine, and degree of cationicity of the tertiary amine on the interfacial properties and performance of cationic polyacrylates were investigated. The results enabled the identification of the key factor that determines the performance of cationic polyacrylates and will also be helpful for the development of agents for the treatment of produced water.

2. Experimental section

2.1 Materials

Methyl acrylate (MA), ethyl acrylate (EA), dimethylaminoethyl methacrylate (DEM), dimethylaminopropylmethacrylamide (DPM), benzyl chloride, azobisisobutyronitrile (AIBN), ethanol, and *n*-tetradecane were analytically pure and were purchased from Shanghai Aladdin Biochemical Technology Co., Ltd. Crude oil was provided by an offshore oilfield (density of 0.9564 g cm⁻³). Cationic polyacrylates were synthesized according to a literature method.¹⁵ Four variables were changed during the synthesis process, namely, acrylate type, tertiary amine type, mass ratio of the acrylate to the tertiary amine, and degree of cationicity of the tertiary amine. The structures of the cationic polyacrylates are shown in Fig. 1.

The number-average molecular weight (M_n), weight-average molecular weight (M_w), and polydispersity index (PDI) of seven representative polymers were determined using a PL-GPC 50 gel permeation chromatograph (Agilent, USA). The gel permeation column was a linear Ultrahydrogel column (7.8 × 300 mm), and distilled water was used as the solvent. The samples were dissolved in water and analyzed at a flow rate of 0.8 mL min⁻¹. The results are listed in Table 1. We found that when polymers had the same degree of cationicity they had similar molecular weights, which were in the range of 33 000–38 000 g mol⁻¹.

2.2 Measurement of surface and interfacial tension

According to our previous study,¹⁵ the surface tension and interfacial tension of an aqueous solution of a cationic polyacrylate decreased to an equilibrium value with an increase in

concentration to 1500 mg L⁻¹ and 50 mg L⁻¹, respectively. In this study, the surface tension of solutions of cationic polyacrylates with a concentration of 1500 mg L⁻¹ was measured at room temperature (flotation was conducted at room temperature) using a DSA30 drop shape analysis system (KRÜSS, Germany). The interfacial tension of solutions of cationic polyacrylates with a concentration of 50 mg L⁻¹ was measured using a TX-500C interfacial tension meter (CNG, USA) at 65 °C (reverse demulsification was conducted at 65 °C).

2.3 Measurement of zeta potential

At 65 °C, the zeta potentials of oil droplets in water before and after reverse demulsification were measured using a ZetaPALS zeta potential analyzer (Brookhaven Corp., USA).

2.4 Measurement of interfacial elastic modulus

The elastic modulus of an oil–water interface is an indicator of the strength of the interfacial film.^{16,17} A DSA30 drop shape analysis system was used to measure the elastic modulus of the interface between cationic polyacrylate solution and oil at 65 °C. During the experiment, the density of the oil phase was 0.8536 g cm⁻³ (the oil phase comprised a mixture of aviation kerosene and crude oil with a mass ratio of 3 : 1), and the oscillation frequency was 0.7 Hz.

2.5 Optical tweezer experiment

The interaction force between two oil droplets is important for the aggregation and coalescence of oil droplets, and optical tweezers are an effective means of measuring the interaction force between two oil droplets. According to a previous study,¹⁸ Tweez 250si optical tweezer (Aresis, Slovenia) was used to measure the interaction force between two tetradecane droplets in water as follows: (1) for the preparation of an oil-in-water emulsion, 95 g pure water and 5 g tetradecane were added to a Waring blender, the stirring speed was adjusted to 7000 rpm, and the mixture was sheared for 10 min; (2) for sample preparation, 1 mL of the oil-in-water emulsion was added to 100 mL of cationic polyacrylate solution (the polymer concentration was 2000 mg L⁻¹) to obtain the sample to be tested; and (3) for the measurement of the interaction force, the sample was injected into the sample cell, and two tetradecane droplets were slowly brought into contact with each other using the linear optical trap and were then slowly separated. This process was analyzed using Tweeze force software to determine the interaction force between the two tetradecane droplets.

2.6 Oil-covered bubble experiment

A collision between an oil droplet and a bubble can be created by an oil-covered bubble experiment.^{19,20} The experimental setup was built according to a literature method.²¹ The oil droplet and bubble were kept in the same vertical line, and the sizes of the oil droplet and bubble were controlled by a micro-injection pump and were 0.8 mm and 1 mm, respectively. The attachment of the oil droplet to the bubble surface was observed by two high-speed cameras. The resulting pictures are shown in



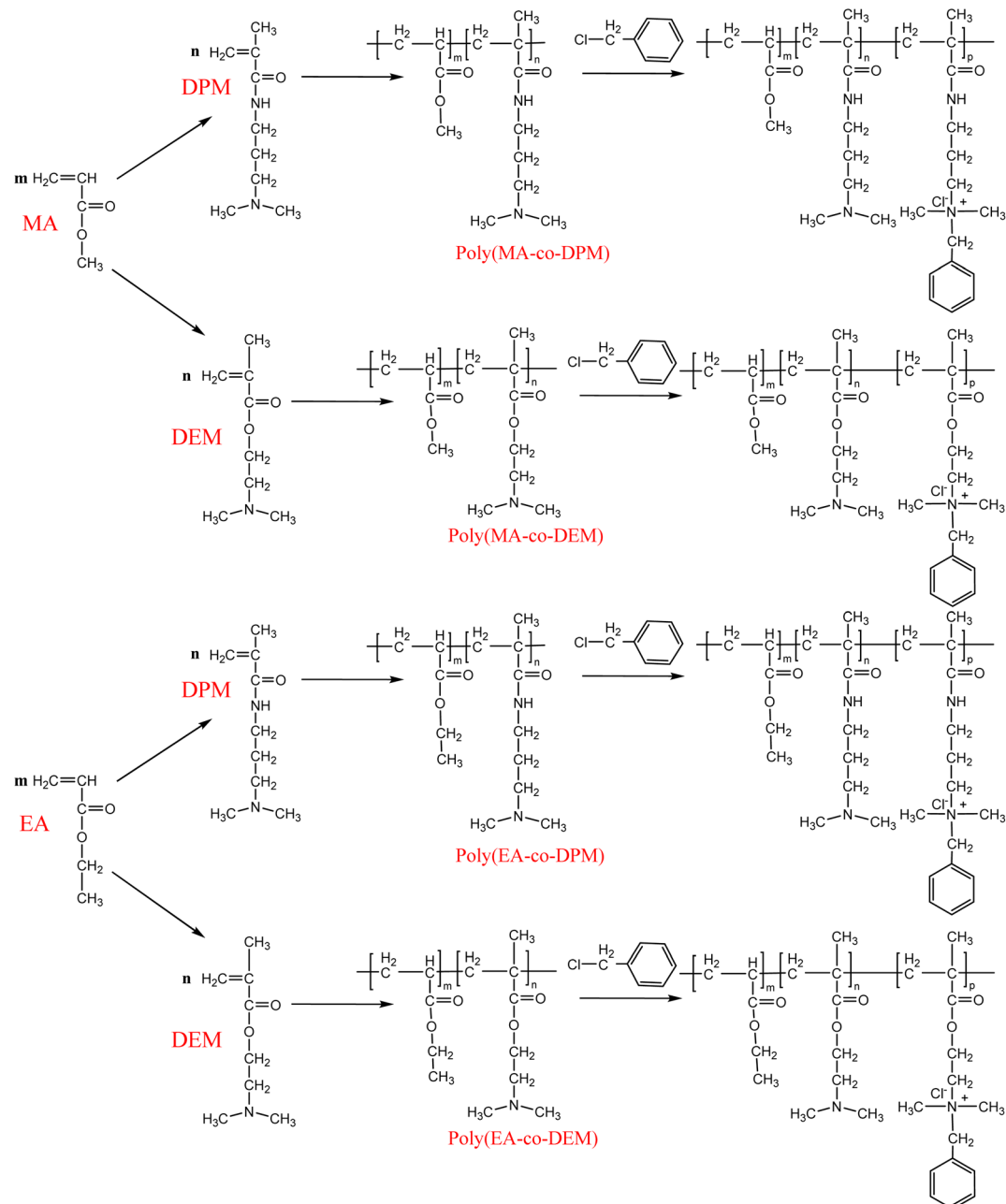


Fig. 1 Structures of different cationic polyacrylates.

Table 1 Molecular weights and molecular weight distributions of representative polymers

Polymer	Composition of structural units	Degree of cationicity of tertiary amine	M_n (g mol ⁻¹)	M_w (g mol ⁻¹)	PDI
Cationic poly(EA-co-DPM)	EA : DPM = 2 : 1	1.0	33 764	57 865	2.122
Cationic poly(EA-co-DPM)	EA : DPM = 2 : 1	0.6	31 374	56 495	1.598
Cationic poly(EA-co-DPM)	EA : DPM = 2 : 1	0.3	27 264	54 335	1.633
Cationic poly(EA-co-DPM)	EA : DPM = 1 : 2	1.0	38 387	62 597	1.631
Cationic poly(EA-co-DPM)	EA : DPM = 1 : 1	1.0	36 679	61 047	1.664
Cationic poly(MA-co-DPM)	MA : DPM = 2 : 1	1.0	31 973	56 095	1.598
Cationic poly(EA-co-DEM)	EA : DEM = 2 : 1	1.0	32 448	56 788	1.475



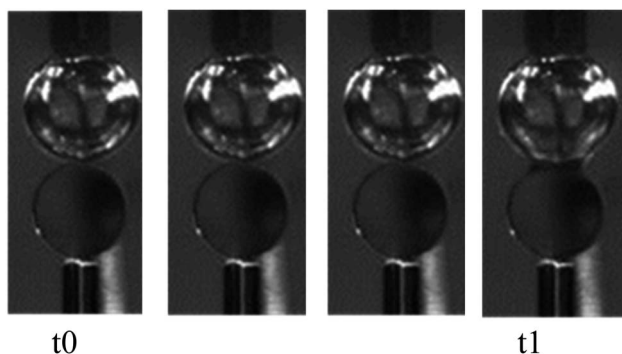


Fig. 2 Process of adhesion of the oil droplet to the bubble surface.

Fig. 2, where the instant of contact between the oil droplet and bubble is defined as t_0 , the moment when the film started to break is defined as t_1 , and the film drainage time t is defined as $t = t_1 - t_0$. The film drainage time determines how easily the oil droplet adheres to the bubble surface. The experiment was conducted at 25 °C.

3. Results and discussion

3.1 Study of structure–property–reverse demulsification performance relationship

When the reverse demulsifier was added to the oil-in-water emulsion, firstly, it diffused from the water to become adsorbed onto the oil–water interface. Then, the properties of the oil–water interface were changed, and the aggregation and coalescence of oil droplets were promoted. Finally, oil–water separation occurred.

3.1.1 Effect of molecular structure on interfacial tension.

When the tertiary amine was DPM and the degree of cationicity of DPM was 1.0, the effects of the type of acrylate and the mass ratio of the acrylate to the tertiary amine on the interfacial tension are shown in Fig. 3(a). When the acrylate was EA and the mass ratio of EA to the tertiary amine was 2 : 1, the effects of the

type of tertiary amine and the degree of cationicity of the tertiary amine on the interfacial tension are shown in Fig. 3(b). The interfacial tension of the polymer prepared from MA and DEM was lower, which indicated that MA and DEM made the polymer exhibit higher interfacial activity. When the mass ratio of the acrylate to the tertiary amine was 2 : 1, the interfacial tension of the polymer was lower than that at the other two ratios, and the interfacial activity was higher. The interfacial tension of the polymer increased with the increase in the degree of cationicity of the tertiary amine, which indicated that the higher was the degree of cationicity of the tertiary amine, the lower was the interfacial activity.

3.1.2 Effect of molecular structure on zeta potential. The zeta potential of an oil droplet before treatment was -25.2 mV. After treatment with 10 mg L $^{-1}$ cationic polyacrylate, the zeta potential of the oil droplet was measured, and the effect of the molecular structure on the zeta potential is shown in Fig. 4. The addition of the cationic polyacrylates significantly reduced the absolute value of the zeta potential, which indicated that the stability of the oil droplet was weakened. Moreover, the absolute value of the zeta potential when EA was used was lower than that when MA was used, and when DPM was used it was lower than that when DEM was used. The absolute value of the zeta potential was significantly lower than that at the other two ratios when the mass ratio of EA to DPM was 1 : 2, whereas the absolute value of the zeta potential decreased with the increase in the degree of cationicity. These results also indicated that the mass ratio of the acrylate to the tertiary amine was the key factor that determined the zeta potential.

3.1.3 Effect of molecular structure on interfacial elastic modulus. The natural components in crude oil can form a strong interfacial film on the surface of oil droplets, which prevents coalescence of the oil droplets and thus results in a stable emulsion.^{22,23} When the tertiary amine was DPM, the mass ratio of the acrylate to DPM was 2 : 1, and the degree of cationicity of DPM was 1.0, the effect of the type of acrylate on the interfacial elastic modulus is shown in Fig. 5(a). When the acrylate was EA, the mass ratio of EA to the tertiary amine was

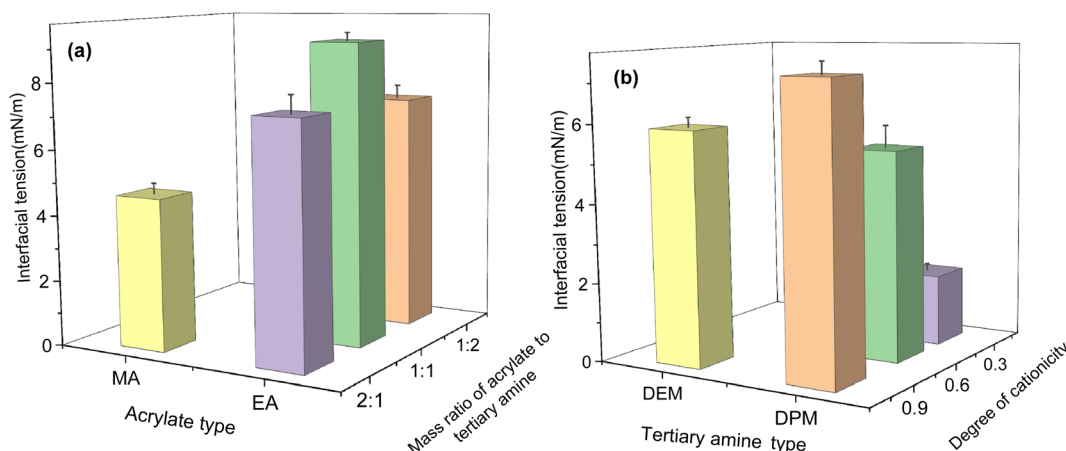


Fig. 3 Effect of molecular structure on interfacial tension: (a) acrylate type and mass ratio of acrylate to tertiary amine; (b) tertiary amine type and degree of cationicity of tertiary amine.

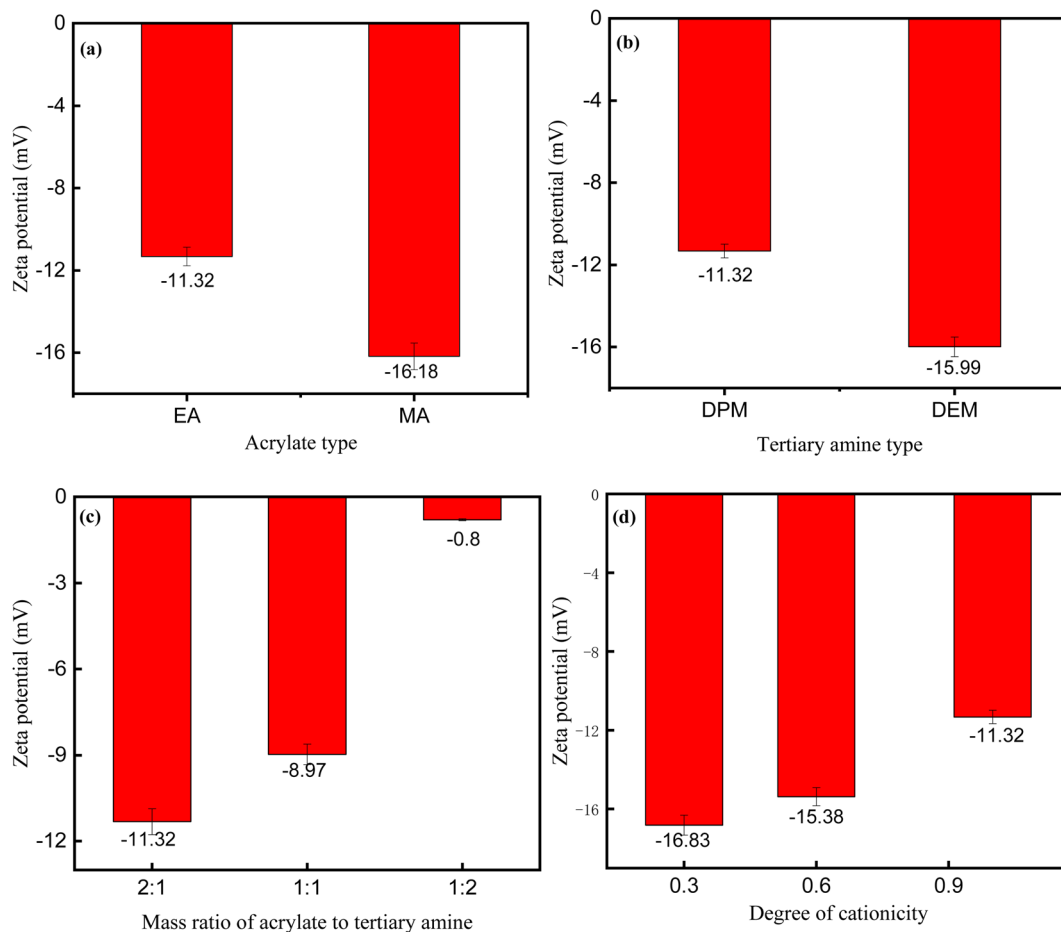


Fig. 4 Effect of molecular structure on zeta potential: (a) acrylate type; (b) tertiary amine type; (c) mass ratio of acrylate to tertiary amine; (d) degree of cationicity.

2 : 1, and the degree of cationicity of the tertiary amine was 1.0, the effect of the type of tertiary amine on the interfacial elastic modulus is shown in Fig. 5(b). When the acrylate was EA, the tertiary amine was DPM, and the degree of cationicity of DPM was 1.0, the effect of the mass ratio of EA to DPM on the interfacial elastic modulus is shown in Fig. 5(c). When the acrylate was EA, the tertiary amine was DPM, and the mass ratio of EA to DPM was 2 : 1, the effect of the degree of cationicity of DPM on the interfacial elastic modulus is shown in Fig. 5(d). The results showed that the copolymer of EA and DPM reduced the interfacial elastic modulus to less than 18 mN m⁻¹ when the polymer concentration was 10 mg L⁻¹, but the copolymer of MA and DEM only reduced it to about 20 mN m⁻¹. These results indicated that the products prepared from EA and DPM formed a lower-strength interfacial film after their adsorption onto the oil–water interface, which made it easier for oil droplets to coalesce and aggregate.²⁴ In addition, when the mass ratio of EA to DPM was 2 : 1, the product was able to reduce the interfacial elastic modulus more substantially than at the other two ratios, which was also beneficial for the coalescence and aggregation of oil droplets. When the degree of cationicity was 0.3, the elastic modulus was only reduced to about 25 mN m⁻¹ at a polymer concentration of 10 mg L⁻¹, which indicated that this low

degree of cationicity was not conducive to the coalescence and aggregation of oil droplets. When the degree of cationicity was increased, the ability of the product to reduce the elastic modulus was significantly enhanced.

3.1.4 Effect of molecular structure on interaction force between oil droplets. The interaction force between oil droplets measured by optical tweezers can indicate the coalescence and aggregation properties of oil droplets.^{25–27} The effect of molecular structure on the interaction force between oil droplets is shown in Fig. 6, where the positive region of the y-axis corresponds to a repulsive force and the negative region of the y-axis corresponds to an attractive force. Usually, the interactions between two oil droplets comprise classical Derjaguin–Landau–Verwey–Overbeek (DLVO) interactions and non-DLVO interactions.^{28,29} DLVO interactions include van der Waals interactions and electrostatic repulsion forces, whereas non-DLVO interactions include hydrophobic forces, steric forces, depletion forces, polymer bridging interactions, and hydration forces. Of these forces, electrostatic forces, hydration forces, and steric forces are repulsive forces, and van der Waals interactions, depletion forces, and polymer bridging interactions are attractive forces. Both EA and MA were able to generate an attractive force between oil droplets that may have been due to polymer



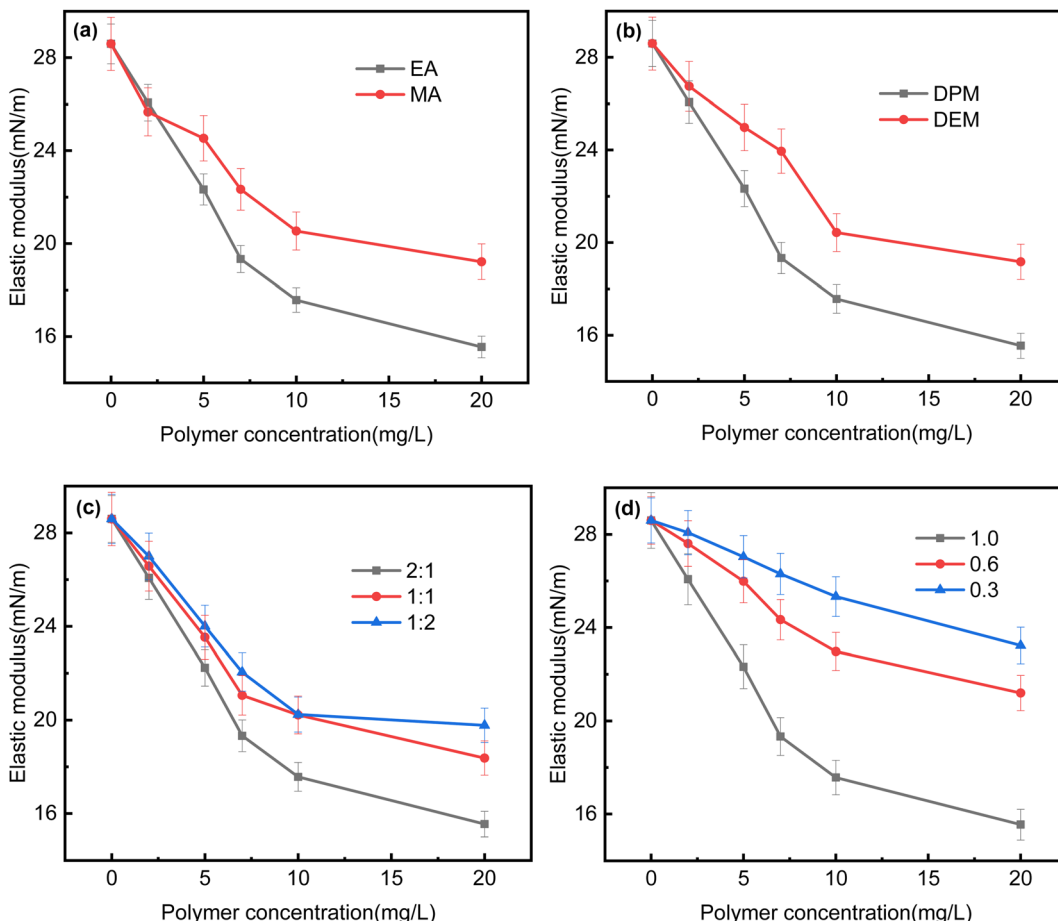


Fig. 5 Effect of molecular structure on elastic modulus: (a) acrylate type; (b) tertiary amine type; (c) mass ratio of acrylate to tertiary amine; (d) degree of cationicity of DPM.

bridging interactions. This indicated that they prolonged the collisional contact time of oil droplets and promoted coalescence and aggregation of oil droplets. MA caused the attractive force between oil droplets to be only about 2 pN, whereas the attractive force between oil droplets caused by EA reached 10 pN, which indicated that EA could make oil droplets collide and aggregate more easily. DEM could not make oil droplets attract each other, and aggregation of oil droplets was therefore more difficult. When the mass ratio of EA to DPM was 1:1, the interaction force between oil droplets was slightly stronger than that at the other two ratios and reached more than 12 pN. The attractive force increased with the increase in the degree of cationicity, which may have been due to a decrease in electrostatic repulsion forces between oil droplets. When the degree of cationicity was 0.3 the attractive force was less than 5 pN, but when the degree of cationicity was 1.0 the attractive force increased to 10 pN, which greatly enhanced the aggregation of oil droplets.

3.1.5 Summary of structure–property–reverse demulsification performance relationship. The results of evaluation of the reverse demulsification performance of different products have been presented in the literature,¹⁵ and the molecular structure–property–reverse demulsification performance relationship is summarized in Fig. 7. We found that among the four

abovementioned properties the elastic modulus of the oil–water interface was the key property that determined the reverse demulsification performance. EA was preferred over MA, and DPM was preferred over DEM. In addition, increases in the mass ratio of EA to DPM and the degree of cationicity of DPM were beneficial for reducing the elastic modulus. Therefore, a higher mass ratio of EA to DPM and a higher degree of cationicity of DPM would lead to better reverse demulsification performance. We speculated on reasons that could explain these results. EA was superior to MA, which may be because EA is more hydrophobic and therefore more easily adsorbed onto the surface of oil droplets to change their interfacial properties. DPM and DEM contain amide and ester groups, respectively. Amide groups have stronger interactions with water, which may make an oil–water interface such as that containing DPM looser and thus more easily damaged. An increase in the mass ratio of EA to DPM was beneficial for enhancing the adsorption of the polymer on the oil–water interface *via* van der Waals forces between EA and crude oil. Moreover, an increase in the degree of cationicity of DPM was beneficial for enhancing the adsorption of the polymer on the oil–water interface *via* electrostatic attraction between the polymer and oil droplets. A higher interfacial adsorption capacity is more conducive to changes in interfacial properties.

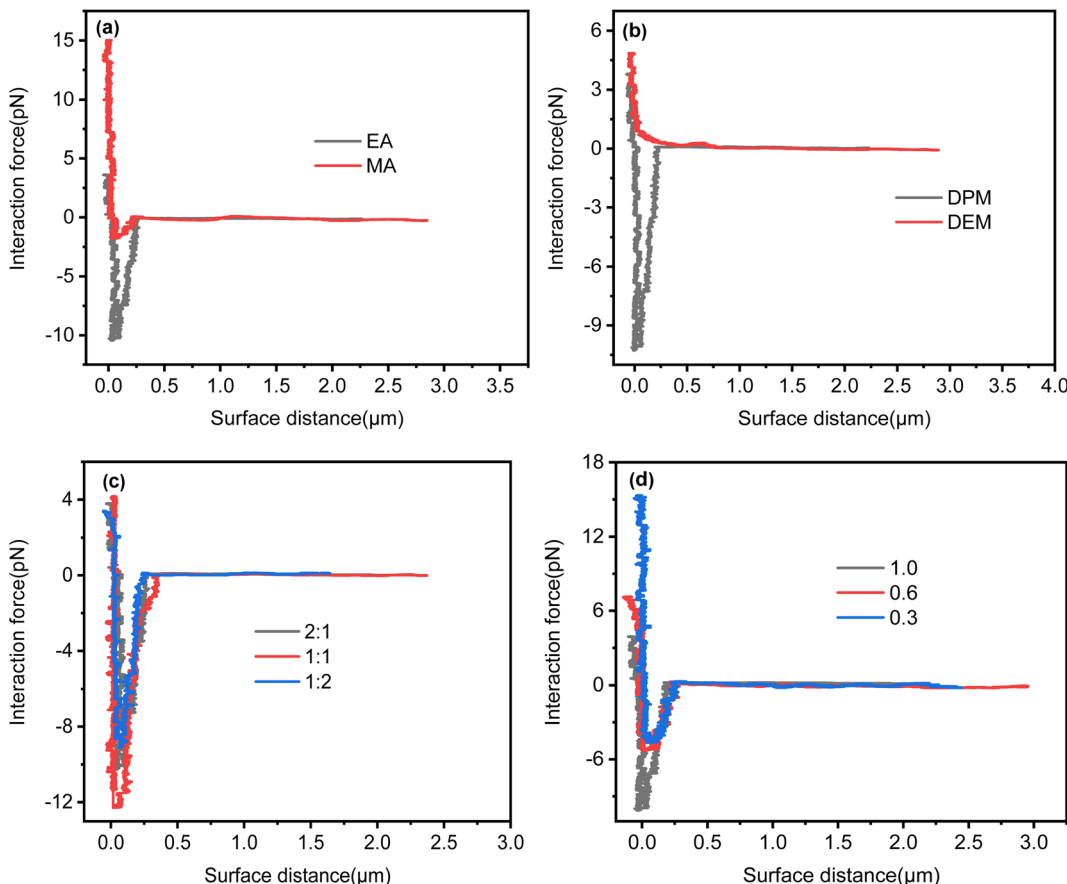


Fig. 6 Effect of molecular structure on attractive force between oil droplets: (a) acrylate type; (b) tertiary amine type; (c) mass ratio of acrylate to tertiary amine; (d) degree of cationicity of DPM (the polymer synthesis conditions were the same as those in Fig. 5).

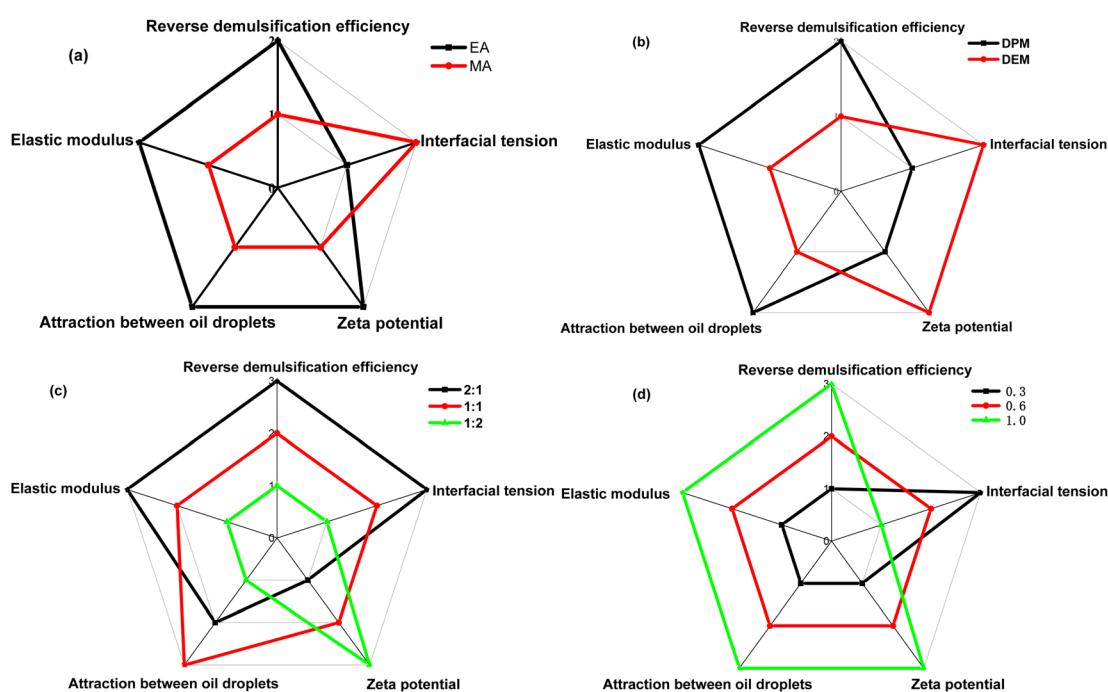


Fig. 7 Relationships between molecular structure, properties, and reverse demulsification performance with regard to: (a) acrylate type; (b) tertiary amine type; (c) mass ratio of acrylate to tertiary amine; (d) degree of cationicity of DPM (1, 2, and 3 represent the magnitude of the property; a larger number indicates a better property).



3.2 Study of structure–property–flotation performance relationship

When the flotation agent was added to the oil-in-water emulsion, it was adsorbed onto the surfaces of oil droplets and air

bubbles, which stabilized the bubbles and assisted the oil droplets to adhere to the bubble surfaces to improve the flotation efficiency.

3.2.1 Effect of molecular structure on surface tension. The effect of molecular structure on surface tension is shown in

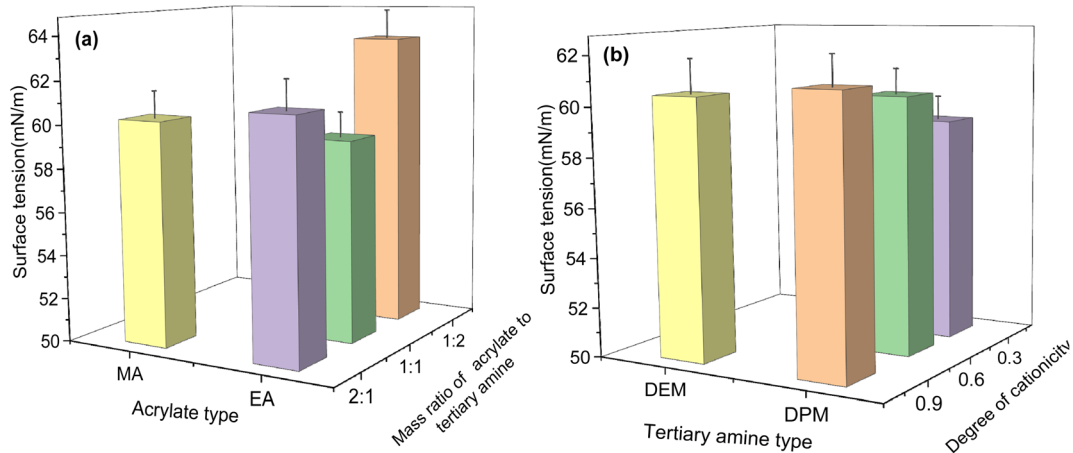


Fig. 8 Effect of molecular structure on surface tension: (a) acrylate type and mass ratio of acrylate to tertiary amine; (b) tertiary amine type and degree of cationicity (the polymer synthesis conditions were the same as those in Fig. 3).

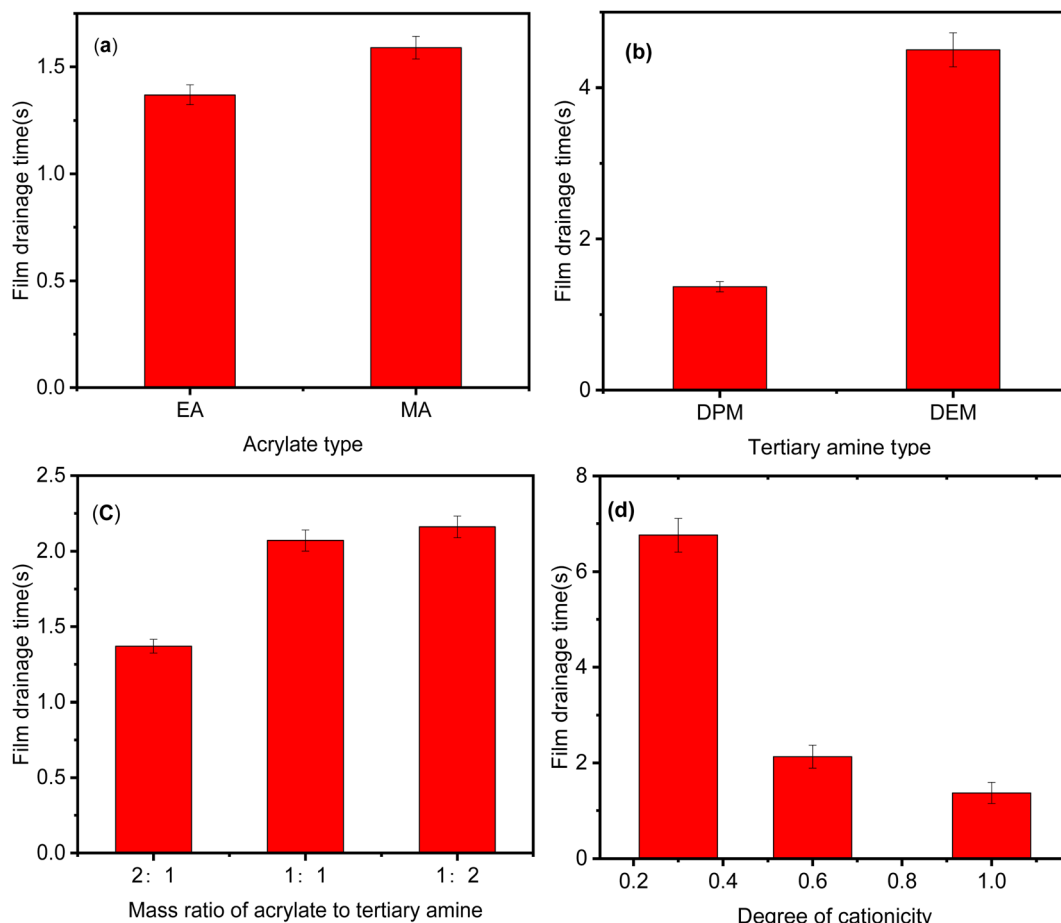


Fig. 9 Effect of molecular structure on film drainage time: (a) acrylate type; (b) tertiary amine type; (c) mass ratio of acrylate to tertiary amine; (d) degree of cationicity (the polymer synthesis conditions were the same as those in Fig. 5).



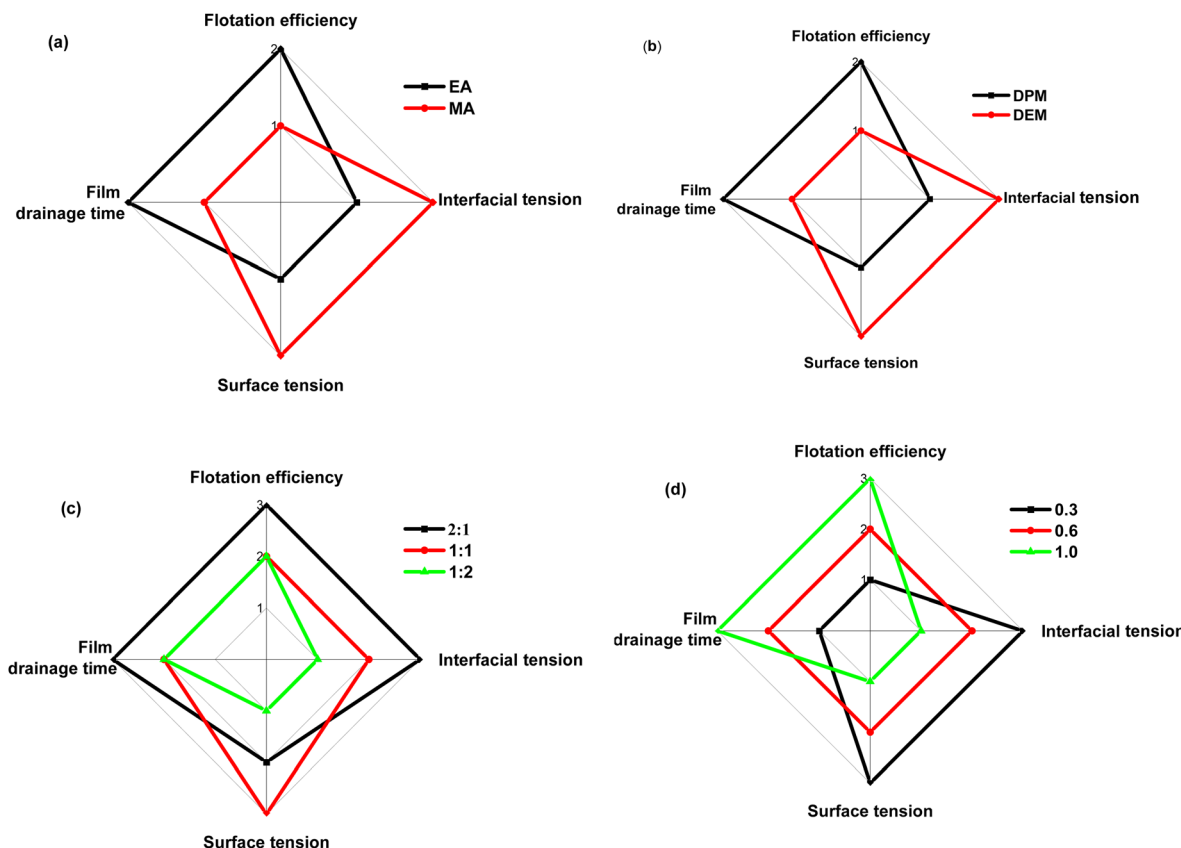


Fig. 10 Relationships between molecular structure, properties, and flotation performance with regard to: (a) acrylate type; (b) tertiary amine type; (c) mass ratio of acrylate to tertiary amine; (d) degree of cationicity of DPM.

Fig. 8. All the polymers were surface-active and could be adsorbed onto the bubble surface, which is the basic property required for air flotation. When the mass ratio of the acrylate to the tertiary amine was 1 : 1, the product was more extensively adsorbed at the gas–liquid interface and had a higher surface activity than at the other mass ratios. In addition, the other structures had the same effect on the surface tension as on the interfacial tension.

3.2.2 Effect of molecular structure on film drainage time. The difficulty with which an oil droplet adheres to a bubble surface depends on the film drainage time,³⁰ and the effect of molecular structure on the film drainage time is shown in Fig. 9. EA had a slightly stronger ability than MA to reduce the film drainage time, which was less than 1.5 s in the case of EA. DEM had a significantly weaker ability than DPM to reduce the film drainage time, which was about 4 s in the case of DEM. These results indicated that the polymers prepared from DPM more easily made the oil droplet adhere to the bubble surface. When the mass ratios of EA to DPM were 1 : 2 and 1 : 1, the two polymers had similar film drainage time. When the mass ratio of EA to DPM was 2 : 1, the ability of the polymer to reduce the film drainage time increased significantly. The film drainage time also decreased as the degree of cationicity increased. The film drainage time was longer than 6.5 s when the degree of cationicity was 0.3 but decreased to less than 1.5 s when the degree of cationicity was increased to 1.0.

3.2.3 Summary of structure–property–flotation performance relationship. The results of evaluation of the flotation performance of different products have been presented in the literature,¹⁵ and the molecular structure–property–flotation performance relationship is summarized in Fig. 10. We found that the film drainage time determined the flotation performance. The ability of the copolymer of EA and DPM to reduce the film drainage time was stronger than that of the copolymer of MA and DEM. In addition, increases in the mass ratio of EA to DPM and the degree of cationicity of DPM were also beneficial for reducing the film drainage time and improving the flotation performance. The reasons for these results may be the same as those proposed in the case of reverse demulsification.

4. Conclusions

The structure–property–performance relationship of cationic polyacrylates was systematically studied in this investigation. The results showed that the surface and interfacial activities of the cationic polyacrylates were the basis of their reverse demulsification and flotation performance. The ability to reduce the oil–water interfacial elastic modulus was the key property for good reverse demulsification performance, and the ability to reduce the film drainage time in the case of oil droplet–bubble adhesion was the key property for good flotation performance. Regarding the selection of the monomer, EA was



superior to MA, and DPM was superior to DEM. This may because the interfacial adsorption capacity of the polymer containing EA was higher and the interfacial film formed by the polymer containing DPM was looser. In addition, increases in the mass ratio of EA to DPM and the degree of cationicity of DPM were beneficial for reducing the oil–water interfacial elastic modulus and film drainage time. This may because increases in the mass ratio of EA to DPM and the degree of cationicity of DPM were beneficial for the interfacial adsorption capacity of the polymer and thus changing the interfacial properties. According to the results, it was found that the cationic polyacrylate with a mass ratio of EA to DPM of 2 : 1 and complete cationization of DPM exhibited good reverse demulsification and flotation performance at the same time. The results of this study provided some useful information for the use of cationic polyacrylates in the treatment of produced water.

Author contributions

Zhiping Chen: investigation, formal analysis, validation. Xiuju Wang: validation. Jian Zhang: validation. Ming Duan: funding acquisition, supervision. Yan Xiong: visualization, writing original draft. Shenwen Fang: conceptualization, methodology, visualization, formal analysis, writing review & editing.

Conflicts of interest

The authors declare that they have no known competing financial interests or personal relationships that could have appeared to influence the work reported in this paper.

Acknowledgements

This work was supported by the National Natural Science Foundation of China (U20B2030 and 52374042) and Key Technologies R&D Program of CNOOC (KJGG2021-0504).

References

- 1 N. Lusinier, I. Seyssiecq, C. Sambusiti, M. Jacob, N. Lesage and N. Roche, Biological treatments of oilfield produced water: A comprehensive review, *SPE J.*, 2019, **24**(5), 2135–2147, DOI: [10.2118/195677-PA](https://doi.org/10.2118/195677-PA).
- 2 M. Al-Salmi, M. Laqbaqbi, S. Al-Obaidani, R. S. Al-Maamari, M. Khayet and M. Al-Abri, Application of membrane distillation for the treatment of oil field produced water, *Desalination*, 2020, **494**, 114678, DOI: [10.1016/j.desal.2020.114678](https://doi.org/10.1016/j.desal.2020.114678).
- 3 M. Golestanbagh, M. Parvini and A. Pendashteh, Integrated systems for oilfield produced water treatment: The state of the art, *Energy Sources, Part A*, 2016, **38**(22), 3404–3411, DOI: [10.1080/15567036.2016.1154903](https://doi.org/10.1080/15567036.2016.1154903).
- 4 J. Zhang, B. Jing, S. Fang, M. Duan and Y. Ma, Synthesis and performances for treating oily wastewater produced from polymer flooding of new demulsifiers based on polyoxyalkylated N,N-dimethylethanolamine, *Polym. Adv. Technol.*, 2015, **26**(2), 190–197, DOI: [10.1002/pat.3433](https://doi.org/10.1002/pat.3433).
- 5 M. Zhang, W. Kang, H. Yang, B. Zhou, Z. Li, Y. He, K. G. Yurievich and L. A. Viktorovich, Demulsification performance and mechanism of β -CD reverse demulsifier for amphiphilic polymer oil in water (O/W) emulsion, *J. Mol. Liq.*, 2021, **342**, 117441, DOI: [10.1016/j.molliq.2021.117441](https://doi.org/10.1016/j.molliq.2021.117441).
- 6 K. Ishak and M. A. Ayoub, Removal of oil from polymer-produced water by using flotation process and statistical modelling, *J. Pet. Explor. Prod. Technol.*, 2019, **9**(4), 2927–2932, DOI: [10.1007/s13202-019-0686-x](https://doi.org/10.1007/s13202-019-0686-x).
- 7 L. Zhang, H. Ying, S. Yan, N. Zhan, Y. Guo and W. Fang, Hyperbranched poly (amido amine) as an effective demulsifier for oil-in-water emulsions of microdroplets, *J. Fuels*, 2018, **211**, 197–205, DOI: [10.1016/j.fuel.2017.09.066](https://doi.org/10.1016/j.fuel.2017.09.066).
- 8 L. Hao, B. Jiang, L. Zhang, H. Yang, Y. Sun, B. Wang and N. Yang, Efficient demulsification of diesel-in-water emulsions by different structural dendrimer-based demulsifiers, *Ind. Eng. Chem. Res.*, 2016, **55**(6), 1748–1759, DOI: [10.1021/acs.iecr.5b04401](https://doi.org/10.1021/acs.iecr.5b04401).
- 9 H. Sun, Q. Wang, X. Li and X. He, Novel polyether-polyquaternium copolymer as an effective reverse demulsifier for O/W emulsions: demulsification performance and mechanism, *Fuel*, 2020, **263**, 116770, DOI: [10.1016/j.fuel.2019.116770](https://doi.org/10.1016/j.fuel.2019.116770).
- 10 Z. Wu, J. Luo and L. Sun, Synthesis and performances for treating oily wastewater of polyether copolymers based on polyethylenimine, *Polym. Adv. Technol.*, 2018, **29**(2), 814–819, DOI: [10.1002/pat.4188](https://doi.org/10.1002/pat.4188).
- 11 J. Zhang, B. Jing, S. Fang, M. Duan and Y. Ma, Synthesis and performances for treating oily wastewater produced from polymer flooding of new demulsifiers based on polyoxyalkylated N,N-dimethylethanolamine, *Polym. Adv. Technol.*, 2015, **26**(2), 190–197, DOI: [10.1002/pat.3433](https://doi.org/10.1002/pat.3433).
- 12 Y. Li, W. Qian, Y. Liu, Y. Li, S. Lu and Q. Hu, Perfluorooctanoic acid (PFOA) removal by flotation with cationic surfactants, *Chemosphere*, 2020, **266**, 128949, DOI: [10.1016/j.chemosphere.2020.128949](https://doi.org/10.1016/j.chemosphere.2020.128949).
- 13 S. Fang, W. Hu, Q. Tang, M. Wang, X. Wang and M. Duan, Synthesis of polytriethanolamine based surfactant and its flotation performance evaluation of oilfield produced water treatment, *J. Dispersion Sci. Technol.*, 2021, **44**, 309–316, DOI: [10.1080/01932691.2021.1947850](https://doi.org/10.1080/01932691.2021.1947850).
- 14 Y. Wang, M. Duan, X. Wang, B. Jing, F. Wang and Y. Xiong, Study of polymerization kinetics and copolymerization behavior of N-[3-(dimethylamino)propyl] methacryamide and cationic surfmers, *J. Appl. Polym. Sci.*, 2020, **137**(47), 49559, DOI: [10.1002/app.49559](https://doi.org/10.1002/app.49559).
- 15 W. Zhang, X. Wang, Y. Wang, Y. Xiong, M. Duan and S. Fang, The effect of cationic unit structure on reverse demulsification and air flotation performance of cationic polyacrylate, *J. Environ. Chem. Eng.*, 2022, **10**(6), 108766, DOI: [10.1016/j.jece.2022.108766](https://doi.org/10.1016/j.jece.2022.108766).
- 16 Z. Wang, X. Lin, T. Yu, N. Zhou, H. Zhong and J. Zhu, Formation and rupture mechanisms of visco-elastic interfacial films in polymer-stabilized emulsions, *J. Dispersion Sci. Technol.*, 2019, **40**(4), 612–626, DOI: [10.1080/01932691.2018.1478303](https://doi.org/10.1080/01932691.2018.1478303).



17 J. Gao, X. Xu, T. Li, H. Zhang, J. Xu and F. Cao, Breakup characteristics of water-in-oil emulsion droplets influenced by a rigid interfacial film in the presence of a polymer surfactant, *Energy Fuels*, 2022, **36**(8), 4339–4347, DOI: [10.1021/acs.energyfuels.2c00313](https://doi.org/10.1021/acs.energyfuels.2c00313).

18 Y. Wang, S. Fang, X. Wang, Y. Xiong and M. Duan, Synthesis of a novel reverse demulsifier with the characteristics of polyacrylate and polycation and its demulsification performance, *J. Appl. Polym. Sci.*, 2021, **138**(41), 51200, DOI: [10.1002/app.51200](https://doi.org/10.1002/app.51200).

19 V. J. Cunningham, E. C. Giakoumatis, M. Marks, S. P. Armes and E. J. Wanless, Effect of morphology on interactions between nanoparticle-stabilised air bubbles and oil droplets, *Soft Matter*, 2018, **14**(17), 3246–3253, DOI: [10.1039/C7SM02280H](https://doi.org/10.1039/C7SM02280H).

20 S. Yan, Y. Zhang, X. Yang, Y. Huang, Z. Bai and X. Xu, Interfacial behavior and internal microflow of an oil droplet during the process of the oil droplet covering a gas bubble: without and with NaCl, *Ind. Eng. Chem. Res.*, 2021, **60**(16), 6006–6015, DOI: [10.1021/acs.iecr.1c00095](https://doi.org/10.1021/acs.iecr.1c00095).

21 Q. Liang, X. Wang, X. Zhang, B. Jing, M. Duan and S. Fang, Comparison of the effects of two flocculants on the interaction between dispersed phases in produced water during air floatation-flocculation, *J. Water Process Eng.*, 2023, **51**, 103483, DOI: [10.1016/j.jwpe.2022.103483](https://doi.org/10.1016/j.jwpe.2022.103483).

22 G. Shu, K. Bu, B. Zhao and S. Zheng, Evaluation of newly developed reverse demulsifiers and cationic polyacrylamide flocculants for efficient treatment of oily produced water, *Colloids Surf. A*, 2021, **51**, 125646, DOI: [10.1016/j.colsurfa.2020.125646](https://doi.org/10.1016/j.colsurfa.2020.125646).

23 Z. Wang, X. Lin, T. Yu, N. Zhou, H. Zhong and J. Zhu, Formation and rupture mechanisms of visco-elastic interfacial films in polymer-stabilized emulsions, *J. Dispersion Sci. Technol.*, 2019, **40**(4), 612–626, DOI: [10.1080/01932691.2018.1478303](https://doi.org/10.1080/01932691.2018.1478303).

24 Z. Li, A. Chakraborty, J. Fuentes, E. Zamora, F. Vázquez, Z. Xu, Q. Liu, C. Flores and W. McCaffrey, Study on demulsifier crude oil interactions at oil-water interface for crude oil dehydration, *Colloids Surf. A*, 2021, **630**, 127526, DOI: [10.1016/j.colsurfa.2021.127526](https://doi.org/10.1016/j.colsurfa.2021.127526).

25 A. Chen, S. Li and J. Xu, A novel approach to study the interactions between polymeric stabilized micron-sized oil droplets by optical tweezers, *Chin. J. Chem. Eng.*, 2020, **28**(5), 1368–1374, DOI: [10.1016/j.cjche.2019.12.010](https://doi.org/10.1016/j.cjche.2019.12.010).

26 A. Chen, Y. Jing, F.-N. Sang, S.-W. Li and J.-H. Xu, Determination of the interaction mechanism of 10 μm oil-in-water emulsion droplets using optical tweezers, *Chem. Eng. Sci.*, 2018, **181**, 341–347, DOI: [10.1016/j.ces.2018.03.012](https://doi.org/10.1016/j.ces.2018.03.012).

27 S. Liu, Y. Hu, J. Xia, N. Li, H. Fan and M. Duan, The attraction between like-charged oil-in-water emulsion droplets induced by ionic micelles, *Colloids Surf. A*, 2022, **654**, 130143, DOI: [10.1016/j.colsurfa.2022.130143](https://doi.org/10.1016/j.colsurfa.2022.130143).

28 J. W. Zhang and H. B. Zeng, Intermolecular and surface interactions in engineering processes, *Engineering*, 2021, **7**, 63–83, DOI: [10.1016/j.eng.2020.08.017](https://doi.org/10.1016/j.eng.2020.08.017).

29 L. Xie, C. Shi, J. Wang, J. Huang, Q. Lu, Q. Liu and H. B Zeng, Probing the interaction between air bubble and sphalerite mineral surface using atomic force microscope, *Langmuir*, 2015, **31**, 2438–2446, DOI: [10.1021/la5048084](https://doi.org/10.1021/la5048084).

30 S. Yan, X. Yang, Z. Bai, X. Xu and H. Wang, Drop attachment behavior of oil droplet-gas bubble interactions during flotation, *Chem. Eng. Sci.*, 2020, **223**, 115740, DOI: [10.1016/j.ces.2020.115740](https://doi.org/10.1016/j.ces.2020.115740).

